Solute effect on strength and formability of Mg: A first-principle study

P. Garg[1], M.A. Bhatia[1], S.N. Mathaudhu[2] and K.N. Solanki[1*]

[1]*School for Engineering of Matter, Transport, and Energy, Arizona State University, Tempe, AZ, USA*
[2]*Mechanical Engineering Department, University of California - Riverside, Riverside, CA, USA*

**(480)965-1869; (480)727-9321 (fax), E-mail: kiran.solanki@asu.edu, (Corresponding author)*

Abstract: In wrought magnesium alloys, room temperature plasticity is largely controlled by limited slip systems such as basal slip and tension/compression twins. The insufficient number of active slip systems limits strength and ductility preventing broader structural applicability of Mg-alloys. Hence, we employ first-principle calculations to investigate the effects of Y and Al alloying elements on shearability and dislocation motion on various slip systems through ideal shear resistance and generalized stacking fault energy calculations. Yttrium is seen to lower the ideal shear resistance and dislocation motion energetics on all the slip systems. On the other hand, aluminum increases the ideal shear resistance but decreases the energy barrier for dislocation motion on various slip systems. The profound effects of solute addition result from the charge transfer between the solute atom and surrounding magnesium atoms.

Keywords: Magnesium; Yttrium; Aluminum; Ideal shear resistance; First principles

1. Introduction

Magnesium (Mg) and its alloys offer great potential for reducing vehicular mass and energy consumption due to their inherently high strength-to-weight ratio (1,2). However, magnesium has poor room temperature formability, which limits its applications when compared with other metallic systems (3). This shortcoming due to a limited number of active slip systems at room temperature (4), leads to failure in wrought polycrystalline Mg-alloys at ambient conditions before sufficient dislocation glide can occur (5,6). However, at high temperatures (> 250°C), non-basal slip systems, such as pyramidal <a> and pyramidal <c+a> slip, can also be activated (5). Thus, to overcome limited ductility, Mg-alloys are generally formed at elevated temperatures (7,8).

In an effort to improve strength and formability at room temperature, recent studies have considered the effects of adding various solute atoms such as Y, Li, Al, Sn and La to Mg (9–13). For instance, Sandlöbes et al. (14) have shown improvement of room temperature ductility in a Mg-3 wt% Y alloy, and suggested the activation of additional pyramidal <c+a> slip as the primary reason for the enhanced ductility. Atomistic methods used by Kim et al. (15) attributed the activation of additional pyramidal <c+a> slip in Mg-Y observed by Sandlöbes et al. (14) to the increase in the critical resolved shear stress (CRSS) of basal slip more than that of non-basal slips, i.e., with the addition of Y, the activation probabilities of basal and pyramidal slip become equal. On the other hand, Stanford et

al. (16), using *in situ* neutron diffraction experiments, have shown that the addition of Y has a strengthening effect on the basal, non-basal <c+a> slip and $\{10\bar{1}2\}$ twinning slip systems resulting in enhanced hardening. For Mg-Al alloys, Valle et al. (17), using electron backscatter diffraction, has shown improvement in ductility due to the activation of prismatic slip and grain boundary sliding. On the other hand, Mg-Al alloys produced using high pressure die casting by Dargusch et al. (18) have lower room temperature ductility due to an increase in the volume fraction of the brittle eutectic phase. First-principles studies by Han et al. (19) show improvement in the ductility of Mg-Al alloys due to a decrease in the stacking fault energy on the basal plane. Whereas, first-principles calculations by Wang et al. (20) show strengthening effect of Al addition to pure Mg due to the formation of strong covalent bonds between Al and Mg atoms. Such divergent experimental and simulation results reflect the ambiguous understanding of the effects of solute addition on the plastic deformation in Mg.

Thus, in the present work, we perform first-principles calculations of ideal shear resistance (τ) for Mg, Mg-Y and Mg-Al alloys along different slip systems (Figures 1a-c) to study the effect of solute addition on shearability. To clarify the entire picture of slip deformation, we compare our ideal shear resistance results with the generalized stacking fault energy (GSFE, γ) values of Pei et al. (21) and Muzyk et al. (22) and propose a new physics-based deformability parameter (δ). Further, to probe the mechanisms associated with the ductility of Mg by solute addition, we analyze the planar charge density distribution on different slip systems in terms of mechanical and chemical contributions at the maximum ideal shear stress and show that the new parameter quantitatively reflects the electronic and atomic response.

2. Computational Technique

Here, ideal shear resistance, which offers fundamental suggestions especially for dislocation nucleation or shearability of the crystal (23), was calculated using the Vienna ab initio simulation package (VASP) based on the density functional theory (DFT) (24). Projector augmented wave (PAW) potentials (25) were used to represent the nuclei core and valence electrons for Mg, Y and Al respectively. Exchange and correlation was treated with the generalized gradient approximation (GGA) using the Perdew-Burke-Ernzerhof (PBE) (26) form with an energy cutoff of 275 eV and the gamma pack k-point mesh of 16 x 9 x 10 was used to perform Brillouin-zone integrations. Note that the 16 x 9 x 10 k-point mesh was selected based on an extensive k-sampling convergences study. For example, the cohesive energy of pure Mg was found to be exactly the same, 1.52 eV/atom, for both k-point meshes of 16 x 9 x10 and 32 x 18 x 20. The quasi-Newtonian method (27) was used to relax the ions with 0.1 meV$Å^{-1}$ force

and 10^{-6} eV energy convergence criteria. Initially, the structural optimization was performed by energy minimization of a pure Mg orthogonal unit cell. Then, we computed the relaxed elastic constants for pure Mg by applying a set of strains with a finite variation of ±0.02 (28). The calculated values of lattice parameters, cohesive energy and elastic constants were all found to be within 5% of the range of experimental values and the reported theoretical values (29). For example, the cohesive energy was found to be 1.52 eV/atom which compares well with the experimental value of 1.51 eV/atom reported by Slutsky and Garland (30). Successful calculation of the equilibrium properties confirms the reliability and accuracy of the preset calculations. Next, the Mg-X (X = Y and Al) solid solution super cell was obtained from a 3 x 3 x 3 unit cell of pure Mg with an X atom substituted for a Mg atom, i.e., 0.93 at. % of X. For the Mg-Al alloy, the energy cut off of 313eV and the gamma pack k-point mesh of 14 x 8 x 9 was used to perform Brillouin-zone integrations. Note that initially we performed cohesive energy calculations using multiple unit cells to obtain a converged unit cell. In this case, the unit cell 3 x 3 x 3 has 108 atoms. The effects of additional atoms within a cell are minimal. For comparison, the cohesive energies of Mg-Y with 108 and 256 atom unit cells were found to be 1.57 and 1.56 eV/atom, respectively. For the ideal shear resistance calculations, the crystal was strained in a series of 0.01 incremental simple shears to obtain the corresponding relaxed and unrelaxed energies. During these calculations, the X atom was free to relax in all directions. VESTA (31) was used for post processing of the charge density data obtained from the DFT simulation to calculate the planar charge density difference contours and to understand the electronic structure of the deformed alloy.

3. Results and discussion

First we focus on the ideal shear resistance of pure Mg, Mg-Y and Mg-Al alloys along different slip systems (Figs 1a-c). Figure 1d and 1e respectively shows the resulting shear stress-strain curves for Mg-Y and Mg-Al alloys along different slip systems, respectively. It is interesting to note that the shear resistance of Mg, Mg-Y and Mg-Al alloys strongly depends on their slip systems and the ideal shear resistance is significantly different among different slip systems. For example, as listed in Table 1, the critical shear resistances (maximum ideal shear stresses) of 1.76 GPa and 1.48 GPa were computed for the basal plane {0001} along both the full dislocation direction $\langle 11\bar{2}0\rangle$ and the partial direction $\langle 10\bar{1}0\rangle$ in Mg, respectively. The calculated critical shear resistance of 1.48 GPa along the basal partial direction in pure Mg is within 4% of previously-simulated values from the literature (1.54 GPa) (29). Note that throughout the paper we refer to the basal full dislocation as a basal and basal partial dislocation as a basal

partial. In the case of prismatic $\{10\bar{1}0\}\langle 11\bar{2}0\rangle$ and pyramidal $\{10\bar{1}1\}\langle 11\bar{2}0\rangle$ slip systems in Mg, the critical shear resistances were found to be 1.58 GPa and 1.62 GPa, respectively.

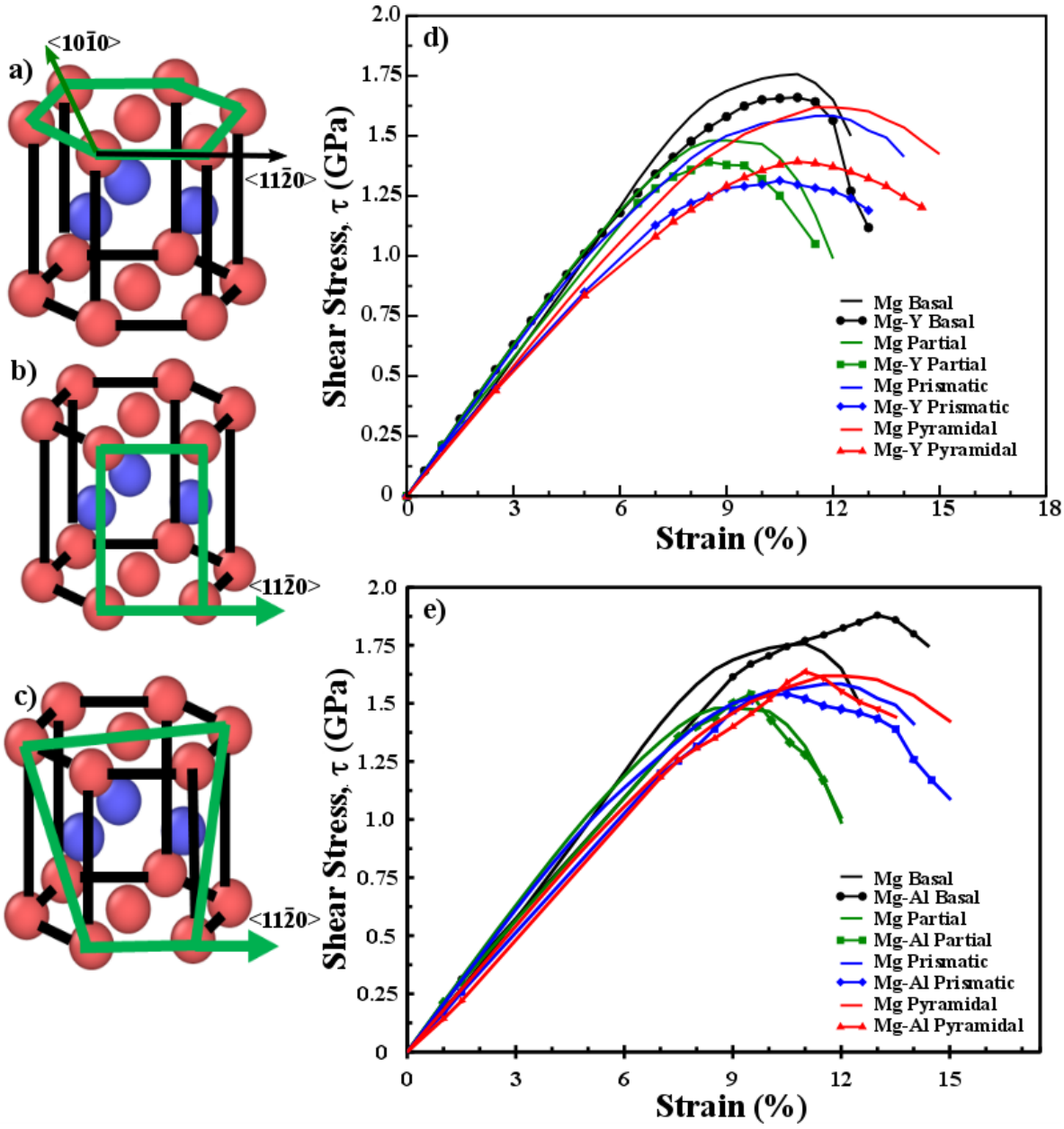

Figure 1: Crystallographic planes of pure Mg (a) basal ($\{0001\}\langle 11\bar{2}0\rangle$) and basal partial ($\{0001\}\langle 10\bar{1}0\rangle$), (b) prismatic ($\{10\bar{1}0\}\langle 11\bar{2}0\rangle$) and (c) pyramidal ($\{10\bar{1}1\}\langle 11\bar{2}0\rangle$) and d) the shear stress – strain responses of pure Mg and Mg-Y alloys and e) the shear stress – strain responses of pure Mg and Mg-Al alloys along different slip systems. Note that throughout the paper we refer to the basal full dislocation as a basal and basal partial dislocation as a basal partial.

Next, we examine the effect of Y and Al respectively on the critical shear resistance behavior of different slip systems in Mg. With the addition of an Y atom, the critical shear resistance for the prismatic slip system decreases from 1.58 GPa to 1.31 GPa, i.e., the addition of an Y atom leads to a decrease in shear resistance of about 17% as compared to the pure Mg. Similarly, the critical shear resistances for the basal, basal partial and pyramidal slip systems were found to decrease by 5%, 6% and 14%, respectively. This behavior shows that Y has a significant beneficial effect on increasing deformability in pure Mg, i.e., with the addition of an Y atom, the shear resistance, which offers fundamental suggestions especially for dislocation nucleation, decreases significantly for each slip system in Mg-Y alloy. The simulations also revealed that with the addition of an Y atom, the shear resistance for the prismatic slip system is lower than that of the basal partial for pure Mg, i.e., shear in the prismatic slip system will occur more readily than shear in the basal partial system with the addition of Y. This behavior has also been observed in recent experiments (14). With the addition of an Al atom, the critical shear resistance for the prismatic slip system decreases from 1.58 GPa to 1.54 GPa, i.e., the addition of an Al atom leads to a small decrease in shear resistance of about 2.5% as compared to the pure Mg. However, the critical shear resistance for the basal, basal partial and pyramidal slip systems was found to increase by 7%, 4% and 2%, respectively. This behavior shows that Al has a detrimental effect on deformability in pure Mg due to strengthening on the basal, basal partial and pyramidal slip systems. The simulations also revealed that with the addition of an Al atom, there is an equal probability of shear on the prismatic and the basal partial slip system since the shear resistance is the same for both the prismatic and basal partial slip systems of the Mg-Al alloy.

In order to obtain a comprehensive view we develop a materials design and performance criteria at the macroscopic level based on the GSFE and shearability. Here, we propose the deformability parameter (δ) which takes into account the relative change in the critical shear resistance and unstable stacking fault energy normalized with their respective elastic constants. If δ is greater than one, the solute addition enhances shearability and dislocation motion. Thus, we define δ based on the critical shear resistance (δ_τ) and GSFE (δ_γ), respectively as:

$$\delta_\tau = (R_\tau)_{Mg-X}/(R_\tau)_{Mg} \qquad \delta_\gamma = (R_\gamma)_{Mg-X}/(R_\gamma)_{Mg} \tag{1}$$

where R_τ and R_γ are the ratios defined for the ideal shear resistance and GSFE, respectively as:

$$R_\tau = [\tau_{BP}/C_{BP}]/[\tau_P/C_P] \qquad R_\gamma = [\gamma^{BP}_{usf}/C_{BP}]/[\gamma^{P}_{usf}/C_P] \tag{2}$$

where τ_{BP}, C_{BP} and γ^{BP}_{usf} are the critical shear resistance, elastic constant and the unstable stacking fault energy for the basal partial slip system, respectively. τ_P, C_P and γ^{P}_{usf} are the critical shear resistance, elastic constant and the

unstable stacking fault energy for the investigated slip plane, respectively. Subscript Mg and Mg-X denotes the investigated planes in a pure Mg and Mg- X, respectively. The R_τ expression can be thought of as an indicator for the solute strengthening, softening or, in general, shearability and the ratio R_γ explain the relative ease of dislocation motion on the corresponding plane as compared to the primary slip plane. The deformability parameter δ for various slip systems are listed in Table 1. It can be seen from Table 1 that the addition of Y enhances shearability and dislocation motion on all the slip systems, when compared with the pure Mg. Addition of Al enhances shearability only on the basal and basal partial slip systems, while dislocation motion is enhanced on various the slip systems by Al addition except prismatic slip when compared to the pure Mg. Further, it is worth emphasizing that these new theoretically formulated predictions are similar to the experimentally observed behavior, as reported in (14). Moreover, we believe that the new parameter quantitatively reflects the electronic and atomic response and, hence, can be used at the macroscopic level for the materials design and selection process.

Table 1. Critical shear stress for different slip systems of Mg and Mg solid solution alloys

	Slip systems	**τ (GPa)**	**γ_{usf} (mJ/m^2)**	**R_τ**	**R_γ**	**δ_τ**	**δ_γ**
Mg-Y	Basal	1.66	214	0.84	0.39	1.16	1.37
	Partial	1.39	83	1.0	1.0	1.0	1.0
	Prismatic	1.31	128	1.01	0.62	1.121	1.63
	Pyramidal	1.39	312	0.87	0.23	1.13	1.03
Mg	Basal	1.76	276	0.73	0.28	-	-
	Partial	1.48	91	1.0	1.0	-	-
	Prismatic	1.58	231	0.90	0.38	-	-
	Pyramidal	1.62	343	0.77	0.22	-	-
Mg-Al	Basal	1.88	252	0.78	0.33	1.07	1.16
	Partial	1.54	83	1.0	1.0	1.00	1.0
	Prismatic	1.54	267	0.78	0.31	0.87	0.82
	Pyramidal	1.65	232	0.62	0.36	0.80	1.60

The mechanical properties of a material are determined by the nature of atomic bonding; therein, both the shear strength and cohesive energy are affected by the directionality and strength of chemical bonds. That is, the non-

uniform distribution of the charge density around an atom gives the indication of bond directionality. For example, the spherical charge density distribution facilitates enhanced shear deformation while a non-spherical charge density distribution hinders shear deformation (32). Further, the anisotropic charge density distribution leads to an elastic anisotropy as shown for FCC Al (32). Therefore, understanding the change in charge density resulting from a solute atom can shed light on the enhanced shearability and dislocation motion in different slip planes. The charge density difference was calculated as:

$$\Delta\rho = \rho_{\mathrm{Mg-X}} - \rho_{\mathrm{Mg}} - \rho_{\mathrm{X}} \quad (4)$$

where $\Delta\rho$ represents the total charge density difference during the deformation, $\rho_{\mathrm{Mg-X}}$ represents the charge density of Mg-X solid solution, and ρ_{Mg} and ρ_{X} represents the charge density of isolated Mg atoms and the X atom, respectively.

Figure 2 illustrates the differential planar charge density in the presence of an Y atom and an Al atom on different slip planes at the maximum ideal shear stress. From these results, we see that the more electronegative Mg attracts the electrons from the Y atom towards itself resulting in the observed softening effect in Mg due to Y addition (Figs. 2a-d). In the case of Y on the basal plane, a non-spherical (anisotropic) and densely distributed charge density distribution was observed (Fig. 2a) as compared to Y on the basal partial plane (Fig. 2b). This correlates with the higher shear resistance that was observed for the basal plane as compared to the basal partial. In the case of non-basal planes such as the prismatic slip plane, the charge accumulation is more spherical and isotropic in nature (Fig. 2c). As a result, a lower critical shear stress (easier to shear) was observed. Figure 2d illustrates the charge density difference in Mg-Y on the pyramidal plane. We notice a slightly higher bond directionality when compared with the prismatic plane charge distribution (Fig. 2c) thereby explaining the higher critical shear stress than in the prismatic slip system.

In general, directional bonding explains the ability of the alloys to accommodate shear deformations, i.e., in this case, distribution of electrons over a larger volume leads to weakening of bonds between Y and Mg atoms which, in turn, decreases the shear resistance of the Mg-Y alloy. Thus, from a broader perspective, we compare our present results with a Mg-Al solid solution which shows enhanced solid solution strengthening (33). Figures 2e-h illustrate the directional bonding (charge density distribution) in the Mg-Al system on different slip planes. From these results, we observed strengthening of bonds due to accumulation of electrons in a smaller volume around the more electronegative Al atom from the surrounding Mg atoms. Alternately, we see the more electronegative Mg attracting

the electrons from an Y atom resulting in the observed softening (Figs. 2a-d). The same behavior of Al in Mg and Y in Mg has been observed experimentally in terms of solid solutions (14,33).

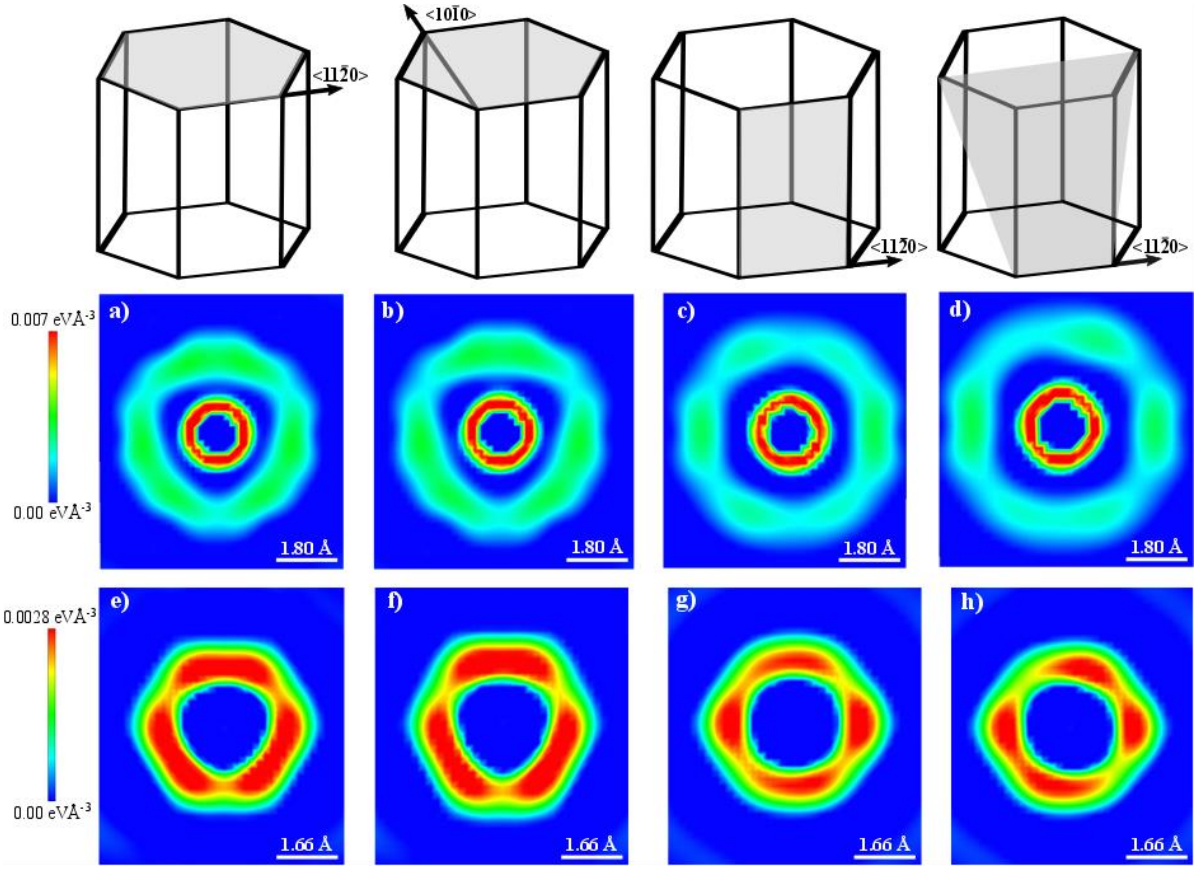

Figure 2: The differential planar charge density (eVÅ^{-3}) in the presence of Y (a-d) and Al (e-h) atoms on different slip planes: a) & e) basal, b) & f) basal partial, c) & g) prismatic and d) & h) pyramidal planes of Mg-Y and Mg-Al alloy, respectively.

Finally, we separate the effect of Y and Al into mechanical (elastic) and chemical (bonding) contributions to the binding energy to gain further understanding of the enhanced behavior of solute addition in Mg. Here, the mechanical contribution was computed by calculating the difference between the energy of relaxed and un-relaxed Mg-X solid solution resulting from structural relaxations with the addition of solute. The chemical contribution was estimated by subtracting the energy of un-relaxed Mg-X solid solution from the energy of relaxed Mg atoms, i.e., the chemical contribution comes from change in energy due to electronic interactions between solutes and surrounding matrix atoms. Table 2 lists the mechanical and chemical contributions of the binding energy due to Y and Al additions in Mg. Comparing the absolute magnitude of the mechanical contribution versus the chemical contribution for both Y and Al solute atoms shows that the mechanical contributions are typically smaller than the

chemical contributions. Therefore, we conclude that, generally, the total energy for the solute softening or strengthening in Mg is dominated by the chemical contribution, resulting in the overall trends in experiments (14,33).

Table 2: The mechanical and chemical contributions to binding energy due to Y and Al addition to Mg, respectively

	Mechanical (eV)	Chemical (eV)	Total (eV)
Mg-Y	-0.002	1.544	1.542
Mg-Al	-0.063	1.641	1.578

4. Conclusion

In conclusion, a systematic first-principles study has been conducted to illustrate the effect of Y and Al solute atoms in Mg-alloys. Our results of ideal shear stress revealed that Y addition lowers the critical shear resistance for all the slip systems in a Mg-Y alloy; whereas, an Al addition increases critical shear resistance on various slip systems, except for the prismatic system. GSFE combined with shearability results allow material design and performance criteria to be formulated at the macroscopic level using a proposed physics-based deformability parameter (δ). The new macroscopic parameter shows that the addition of Y enhances shearability and dislocation motion on different slip systems of the Mg-Y alloy. Al addition enhances shearability on basal and basal partial slip systems while diminishing shearability on the prismatic and pyramidal slip systems in the Mg-Al alloy. Dislocation motion is enhanced on various slip systems of the Mg-Al alloy, except for the prismatic system, when compared with the pure Mg. Further, it is worth emphasizing that these new theoretically formulated predictions are similar to experimentally observed behavior, as reported in (14). Also, the improvement in ductility is due to a variation in bonding characteristics of Mg-Y. Finally, by analyzing the charge density variation we show that the new parameter quantitatively reflects both the electronic and atomic response and, therefore, can be used at the macroscopic level for the materials design and selection process.

References

1. Friedrich H, Schumann S. Research for a “new age of magnesium” in the automotive industry. J Mater Process Technol. 2001;117(3):276–81.
2. Luo AA. Recent magnesium alloy development for automotive powertrain applications. In: Materials Science Forum. Trans Tech Publ; 2003. p. 57–66.

3. Pollock TM. Weight Loss with Magnesium Alloys. Science. 2010 May 21;328(5981):986–7.

4. Christian JW, Mahajan S. Deformation twinning. Prog Mater Sci. 1995;39(1–2):1–157.

5. Yoo M. Slip, twinning, and fracture in hexagonal close-packed metals. Metall Trans A. 1981;12(3):409–418.

6. Yoo MH, Morris JR, Ho KM, Agnew SR. Nonbasal deformation modes of HCP metals and alloys: Role of dislocation source and mobility. Metall Mater Trans A. 2002 Mar 1;33(3):813–22.

7. Park J, Kim H, Ahn S, Chang Y. A study on the boss forming process of AZ31 Mg alloy sheet. Met Mater Int. 2009 Jun 1;15(3):515–20.

8. Lee B, Kim S, Mehtedi M, Evangelista E, Lee C. Effect of stress state on the high temperature workability of AZ31 Mg alloy. Met Mater Int. 2010 Apr 1;16(2):197–203.

9. Sandlöbes S, Friák M, Zaefferer S, Dick A, Yi S, Letzig D, et al. The relation between ductility and stacking fault energies in Mg and Mg–Y alloys. Acta Mater. 2012 Apr;60(6–7):3011–21.

10. Sandlöbes S, Zaefferer S, Schestakow I, Yi S, Gonzalez-Martinez R. On the role of non-basal deformation mechanisms for the ductility of Mg and Mg–Y alloys. Acta Mater. 2011 Jan;59(2):429–39.

11. Agnew S, Yoo M, Tome C. Application of texture simulation to understanding mechanical behavior of Mg and solid solution alloys containing Li or Y. Acta Mater. 2001;49(20):4277–4289.

12. Stanford N, Barnett MR. The origin of “rare earth” texture development in extruded Mg-based alloys and its effect on tensile ductility. Mater Sci Eng A. 2008 Nov;496(1–2):399–408.

13. Bhatia MA, Mathaudhu SN, Solanki KN. Atomic-scale investigation of creep behavior in nanocrystalline Mg and Mg–Y alloys. Acta Mater. 2015 Oct 15;99:382–91.

14. Sandlöbes S, Friák M, Zaefferer S, Dick A, Yi S, Letzig D, et al. The relation between ductility and stacking fault energies in Mg and Mg–Y alloys. Acta Mater. 2012 Apr;60(6–7):3011–21.

15. Kim K-H, Jeon JB, Kim NJ, Lee B-J. Role of yttrium in activation of 〈c+a〉 slip in magnesium: An atomistic approach. Scr Mater. 2015 Nov;108:104–8.

16. Stanford N, Atwell D, Beer A, Davies C, Barnett MR. Effect of microalloying with rare-earth elements on the texture of extruded magnesium-based alloys. Scr Mater. 2008 Oct;59(7):772–5.

17. Del Valle JA, Pérez-Prado MT, Ruano OA. Deformation mechanisms responsible for the high ductility in a Mg AZ31 alloy analyzed by electron backscattered diffraction. Metall Mater Trans A. 2005;36(6):1427–1438.

18. Dargusch MS, Pettersen K, Nogita K, Nave MD, Dunlop GL. The effect of aluminium content on the mechanical properties and microstructure of die cast binary magnesium-aluminium alloys. Mater Trans. 2006;47(4):977–982.

19. Han J, Su XM, Jin Z-H, Zhu YT. Basal-plane stacking-fault energies of Mg: A first-principles study of Li-and Al-alloying effects. Scr Mater. 2011;64(8):693–696.

20. Wang C, Han P, Zhang L, Zhang C, Yan X, Xu B. The strengthening effect of Al atoms into Mg–Al alloy: A first-principles study. J Alloys Compd. 2009 Aug;482(1–2):540–3.

21. Pei Z, Zhu L-F, Friák M, Sandlöbes S, Pezold J von, Sheng HW, et al. Ab initio and atomistic study of generalized stacking fault energies in Mg and Mg–Y alloys. New J Phys. 2013 Apr 1;15(4):43020.

22. Muzyk M, Pakiela Z, Kurzydlowski KJ. Generalized stacking fault energy in magnesium alloys: density functional theory calculations. Scr Mater. 2012;66(5):219–222.

23. Shang SL, Wang WY, Zhou BC, Wang Y, Darling KA, Kecskes LJ, et al. Generalized stacking fault energy, ideal strength and twinnability of dilute Mg-based alloys: A first-principles study of shear deformation. Acta Mater. 2014 Apr;67:168–80.

24. Kresse G, Hafner J. Ab initio molecular dynamics for liquid metals. Phys Rev B. 1993;47(1):558.

25. Blöchl PE, Jepsen O, Andersen OK. Improved tetrahedron method for Brillouin-zone integrations. Phys Rev B. 1994;49(23):16223.

26. Blöchl PE. Projector augmented-wave method. Phys Rev B. 1994;50(24):17953.

27. Pulay P. Convergence acceleration of iterative sequences. The case of SCF iteration. Chem Phys Lett. 1980;73(2):393–398.

28. Jiang L, Muthegowda N, Bhatia MA, Migliori A, Solanki KN, Chawla N. Full elastic constants of Cu6Sn5 intermetallic by Resonant Ultrasound Spectroscopy (RUS) and ab initio calculations. Scr Mater. 2015 Oct;107:26–9.

29. Fu L, Zhang Q, Tang BY. First-Principles Study on the Ideal Strengths of Typical Hcp Metals. In: Advanced Materials Research [Internet]. Trans Tech Publ; 2012 [cited 2015 Nov 11]. p. 2523–2529. Available from: http://www.scientific.net/AMR.476-478.2523

30. Slutsky LJ, Garland CW. Elastic constants of magnesium from 4.2 K to 300 K. Phys Rev. 1957;107(4):972.

31. Momma K, Izumi F. *VESTA* : a three-dimensional visualization system for electronic and structural analysis. J Appl Crystallogr. 2008 Jun 1;41(3):653–8.

32. He R-H, Hashimoto M, Karapetyan H, Koralek JD, Hinton JP, Testaud JP, et al. From a Single-Band Metal to a High-Temperature Superconductor via Two Thermal Phase Transitions. Science. 2011 Mar 25;331(6024):1579–83.

33. Caceres C, Rovera D. Solid solution strengthening in concentrated Mg–Al alloys. J Light Met. 2001;1(3):151–156.